Impact of Electronic Asymmetry on Photoexcited Triplet-State Spin Distributions in Conjugated Porphyrin Oligomers Probed via EPR Spectroscopy

Paul J. Angiolillo*

Department of Physics, Saint Joseph's University, 5600 City Avenue, Philadelphia, Pennsylvania 19131

H. Tetsuo Uyeda, Timothy V. Duncan, and Michael J. Therien*

Department of Chemistry, 231 S. 34th Street, University of Pennsylvania, Philadelphia, Pennsylvania 19104

Received: January 14, 2004

The photophysics of triplet excitons in a series of electronically asymmetric "push−pull" π-conjugated *meso*-to-*meso* ethyne-bridged (porphinato)metal oligomers, along with electronically symmetric analogues, were studied by X-band electron paramagnetic resonance (EPR) spectroscopy under continuous-wave (CW) optical pumping conditions in the 4−100 K temperature range. In all of the systems studied, the spatial extent of the triplet wave function, as inferred from the $|D|$ zero-field splitting (ZFS) parameter, never exceeds the dimensions of a single porphyryl moiety and its *meso*-pendant ethynyl groups. The $|D|$ values determined for an oligomeric series of these electronically asymmetric species that span one through four porphyryl units are respectively 0.0301, 0.0303, 0.0300, and 0.0301 cm^{-1}, indicating a common triplet wave function spatial delocalization of approximately 0.4−0.45 nm. Electron spin−spin and spin−lattice relaxation times were determined over the 4−30 K temperature range using progressive microwave power saturation for benchmark, structurally related electronically symmetric conjugated porphyrin species which possessed either terminal electron-rich [4-dimethylamino(phenyl)]ethynyl or electron-poor [4-nitro(phenyl)]ethynyl substituents. The spin−lattice relaxation times obtained from these experiments reveal no significant scaling of this parameter with conjugation length, consistent with a $S = 1$ spin system that is confined to a single monomeric porphyrin unit and its pendent ethynyl substituents. These results are discussed within the global context of a broader body of experiments that have probed the extent of triplet exciton delocalization within a number of families of highly π-conjugated organic oligomers and polymers.

I. Introduction

Ever since Robbins observed the photoexcited triplet state of single-crystal polydiacetylene,[1] the $S = 1$ spin state has been probed in a wide range π-conjugated organic oligomeric and polymeric materials.[2−15] As such electronic states bear directly upon a diverse array of technologically important processable materials, great effort has been expended to understand (i) the role of the triplet exciton in controlling electro- and photoluminescence quantum efficiency, (ii) the nature of nonlinear optical (NLO) properties manifest by the excited triplet states of electronically asymmetric π-conjugated oligomers, and (iii) the conjugation-length-dependent interplay between singlet and triplet exciton formation as a function of π-conjugated oligomeric and polymeric electronic structure.[16] Conjugated oligomeric arrays featuring porphyrins and related macrocycles that exploit a wide range of linkage motifs (alkynyl, aryl, vinyl, or alkyl units) define structures that can function as optical limiters,[17] optoelectronic gates,[18] molecular and photonic wires,[19,20] and NLO materials.[21−26] Of the aforementioned classes of conjugated oligomers, multiple porphyrin moieties coupled via a *meso*-to-*meso* ethynyl bridging motif define well-characterized oligomeric arrays that feature unprecedented inter-chromophore electronic interactions.[27] Photoexcitation of such species that possess high symmetry produces singlet exciton states that are highly delocalized.[27−32] EPR spectroscopic studies and time-resolved microwave conductivity measurements on analogous triplet exciton states of such species are consistent with triplet excitons that are severely restricted spatially.[30,33−36] Benchmark CW EPR spectroscopic studies that interrogated electronically symmetric *meso*-to-*meso* ethyne and butadiyne-bridged porphyrin oligomers demonstrate that the spatial extent of the electronically excited triplet spin distribution is on the order of 0.4 nm, indicating triplet exciton confinement to a single porphyrin unit and its *meso*-pendant cylindrically π-symmetric substituents (ethyne or butadiyne). Remarkably, triplet exciton confinement in these systems has been shown to be temperature independent from 4 K through to glass transition temperature (∼120 K).[36,37] Related experiments probing triplet excitation confinement in a series of oligomeric alkylthiophenes implicates this phenomenon in the conjugation-length dependence of the electroluminescence quantum efficiency in OLEDs that possess singlet exciton formation efficiencies in excess of the spin-statistical limit of 25%.[3]

The introduction of electron donor (D) and acceptor (A) groups coupled directly to the *meso*-position termini of such conjugated porphyrin oligomers via an ethynyl bridging moiety provides the electronically asymmetric species **1**−**4** highlighted in Figure 1. Attachment of electronically asymmetric arylethynyl units to the antipodal *meso* extrema expands conjugation relative to the respective parent porphyrin-based structures of **1**−**4**, and augments both the transition moment magnitude and excited-singlet polarization (vide infra) relative to these related elec-

* Corresponding authors. E-mail: pangioli@sju.edu. therien@a.chem.upenn.edu.

10.1021/jp040032z CCC: $27.50
Published on Web 07/20/2004

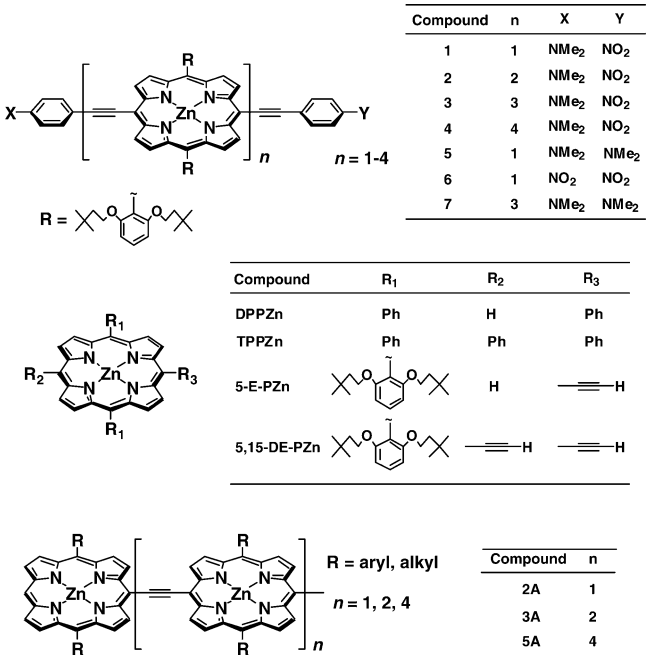

Figure 1. Structures of electronically asymmetric, conjugated *meso*-to-*meso* ethyne-bridged porphyrin oligomers featuring terminal aryl-ethynyl moieties along with key reference compounds.

tronically symmetric benchmarks [**DPPZn**, **2A**, **3A**, and **5A**] highlighted in Figure 1.[24,27,29,30,32,33,36,38,39]

This paper explores the impact of electronic asymmetry upon the nature of lowest-lying triplet excited-state wave function in *meso*-ethyne-bridged porphyrin arrays, and probes whether this electronic structural modification in highly π-conjugated oligomers drives perturbations to the triplet exciton state similar to that effected in the corresponding singlet exciton wave function. In these systems, we determine the triplet spin distribution from an analysis of the zero-field splitting (ZFS) parameters and electron spin−lattice relaxation (SLR) times extracted from EPR spectra of the optically pumped triplet states of these compounds obtained within frozen glassy matrices. Analysis of these data suggests that a universal trend exists with respect to strong localization of triplet excitation within these highly conjugated organic materials; these results are further discussed within the global context of a broader body of experiments that have probed the extent of triplet exciton delocalization within other classes of highly π-conjugated organic oligomers and polymers.

II. Experimental Section

Details describing the synthesis of the compounds used in this study will be reported elsewhere.[40] Electronic spectra were obtained on an OLIS UV/vis/NIR spectrophotometer that is based on the optics of a Cary 14 spectrophotometer. Emission spectra were recorded on a Spex Fluorolog 3-211 spectrophotometer fitted with a Hammamatsu red-sensitive R2658 photomultiplier detector and a liquid-nitrogen cooled InGaAs detector, both of which were corrected for their spectral response against a National Institute of Standards and Technology (NIST) calibrated lamp.

Electron paramagnetic spectroscopy experiments were performed on Brüker ESP 300E and Varian E-109 spectrometers. Optical pumping of the triplet manifold was accomplished through intracavity excitation via a fiber optic cable utilizing a 150 W quartz-halogen excitation source (Kuda, Mitsubishi Corp.). Appropriate filtration of infrared radiation was accomplished using a Corning blue heat filter. Temperatures were maintained utilizing an Oxford ESR 900 continuous flow liquid helium cryostat regulated with an Oxford ITC4 temperature controller; using this system, temperatures reported herein are accurate within ± 1 K over the temperature ranges studied. Microwave frequency was determined using a Hewlett-Packard 5350B frequency counter (Brüker) or an EIP model 351 frequency counter (Varian). All experiments were conducted at microwave powers (2−10 μW) that ensured that resonance saturation did not occur. EPR spectra of the optically pumped triplet states were obtained through numerical subtraction of spectra obtained without irradiation from those obtained during irradiation. Optical absorption spectra of all compounds were obtained after EPR spectral collection in order to assess compound integrity; no evidence of photodegradation was ever observed for any sample examined in this study. Electron spin lattice relaxation (SLR) times were determined using progressive microwave power saturation. The spectral intensity maxima of the canonical transitions (Z_I and Z_{II}) as a function of the square root of the microwave power were analyzed using the methods described by Wheeler et al.[41]

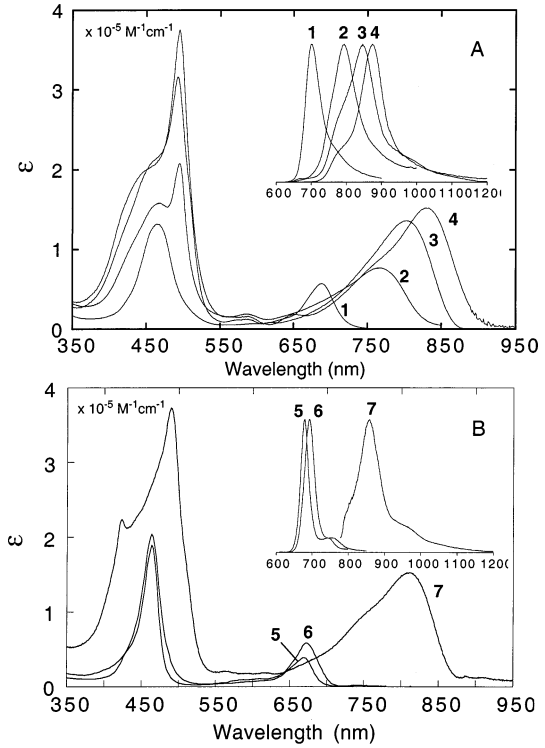

Figure 2. Linear absorption spectra of electronically asymmetric compounds **1**−**4** (A) and electronically symmetric compounds **5**−**7** (B) in tetrahydrofuran solvent at 298 K. The insets show the normalized fluorescence emission spectra; electronic excitation energies were restricted to the red edge of the Q-band absorption envelope of these compounds.

III. Results and Discussion

A. Linear Absorption and Emission Spectroscopy. Figure 2 displays the linear absorption and fluorescence emission spectra for compounds **1**−**7** and provides a context within which to contrast corresponding triplet state photophysical phenomena; a detailed analysis of these data will be reported elsewhere.[40] Several notable trends are exhibited in the singlet-state spectroscopy delineated for **1**−**4**. The linear electronic absorption spectra of these compounds are dominated by two visible absorption manifolds, that define the Q ($S_0 \rightarrow S_1$) and B (Soret)

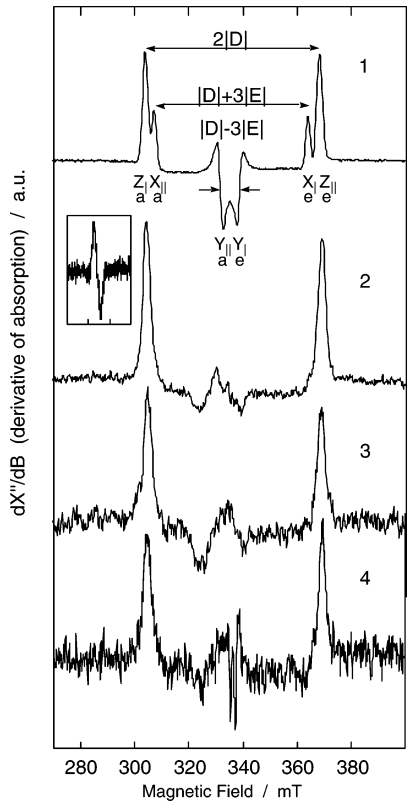

Figure 3. X-band EPR spectra of the optically pumped lowest-energy triplet excited states of compounds **1**−**4** at 4 K. The inset to the spectrum obtained for compound **2** shows the half-field ($|\Delta M_s| = 2$) resonance. Experimental conditions: microwave power = 10 mW; modulation amplitude = 2 mT at 100 kHz; sample concentration ~ 1 mM; solvent = 10:1 toluene:pyridine.

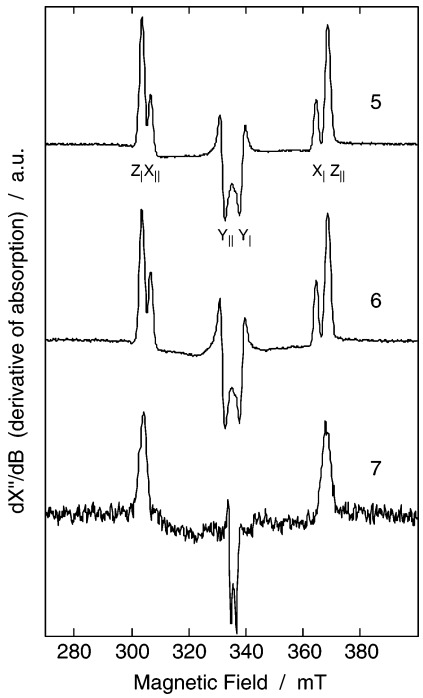

Figure 4. X-band EPR spectra of the optically pumped, lowest-energy triplet excited states of compounds **5**−**7** at 4 K. Experimental conditions: microwave power = 10 mW; modulation amplitude = 2 mT at 100 kHz; sample concentration ~1 mM; solvent = 10:1 toluene: pyridine.

band ($S_0 \rightarrow S_2$) spectral domains. The $S_0 \rightarrow S_1$ transition energy (determined from the low energy absorption maxima of Figure 2 spectra) of compounds **1**−**4** scales with increasing conjugation length; energies associated with this absorption are 1.80, 1.62, 1.54, and 1.49 eV, respectively, for **1**−**4**. This trend, along with the fact that there is a dramatic concomitant increase in the oscillator strength and red shift of the lower energy Q-state absorption manifold with increasing conjugation length (Figure 2), indicates that the *meso*-to-*meso* ethynyl linkage motif effects significant frontier orbital dispersion with respect to monomeric porphyrinic building blocks, and highlights that $^1(\pi-\pi^*)$ excitation is effectively globally delocalized in these species over conjugation lengths of this magnitude. The spectral breadth of the high-energy $S_0 \rightarrow S_2$ transition manifold, along with the energetic separation of the two prominent transitions in this region for oligomers **2**−**4**, scale also with conjugation length. These gross spectral features, which evince the hallmarks of extensive π conjugation and exciton coupling, have been analyzed in detail for a wide range of structurally related compounds.[24,27−33,36,38,39,42,43]

The fluorescence emission ($S_0 \leftarrow S_1$) spectra of compounds **1**−**4** closely mirror that of the lowest-energy $S_0 \rightarrow S_1$ absorptions, displaying emission band maxima located at 1.77, 1.56, 1.47, and 1.42 eV and exhibiting Stokes' shifts of 30, 60, 70, and 70 meV, respectively (Figure 2 inset). These exceedingly small Stokes' shifts are commensurate with the globally delocalized nature of the S_1 state, and the correspondingly small nuclear displacements manifest in the electronically excited states of these species relative to their respective ground-state nuclear coordinates. Compounds **1**-**4** do not exhibit any obvious ambient-temperature phosphorescence ($S_0 \leftarrow T_1$) emission; previous photophysical studies interrogating *meso*-ethyne elaborated monomeric porphyrins have shown, however, a clear 0−0 phosphorescence emission ($\lambda_{S_0 \leftarrow T_1} \sim 815-900$ nm) that has an associated vibronic band approximately 170 meV to the red.[36]

B. Photoexcited Triplet EPR Spectroscopy. To gain insight into how electronic asymmetry affects the distribution of excitation energy within the triplet manifold of D- and A-derivatized *meso*-to-*meso* ethyne-bridged porphyrin arrays, the lowest photoexcited triplet states of unoriented samples of **1**−**7** were studied by EPR spectroscopy in glassy solvent systems at low temperature (4−100 K) under continuous broad-band visible light irradiation. The results are shown in Figures 3 and 4. The shape of the EPR spectrum of randomly oriented molecules in their excited triplet state depends on the zero-field splitting (ZFS) parameters, and on entry, exit, and spin−lattice relaxation rates of the triplet spin sublevels. The EPR spectrum of a $S > {}^1/_2$ spin system is governed in general by the spin Hamiltonian

$$H = \beta_e \mathbf{B}\cdot\bar{\bar{\mathbf{g}}}\cdot\mathbf{S} + \mathbf{S_1}\cdot\bar{\bar{\mathbf{J}}}\cdot\mathbf{S_2} \qquad (1)$$

where the first term is the typical electron Zeeman interaction and the second term is the spin−spin interaction term, where $\vec{S}$ is the total spin, S_1 and S_2 are the spins of the interacting centers, $\bar{\bar{g}}$ is the *g*-factor tensor, **B** is the applied magnetic field field, and β_e is the electron Bohr magneton.[44] $\bar{\bar{\mathbf{J}}}$ is a second-rank tensor that contains all the relevant interaction parameters, which is typically decomposed into three terms: $J_o\mathbf{S_1}\cdot\mathbf{S}_2 + d_{12}\mathbf{S_1} \times \mathbf{S}_2 + \mathbf{S}_1\cdot\bar{\bar{\mathbf{D}}}\cdot\mathbf{S_2}$.[45] The first term is the isotropic exchange interaction; it is generally omitted in discussion of the triplet state since it affects only the energy separation of the singlet and triplet manifolds. The second term is the antisymmetric spin−spin interaction which vanishes for the triplet manifold. The last term is the generalized anisotropic electron−electron spin interaction where $\bar{\bar{\mathbf{D}}}$ is a symmetric, traceless tensor. Thus, for $S = 1$ spin states, the Hamiltonian takes the form

$$H = \beta_e \mathbf{B}\cdot\bar{\bar{\mathbf{g}}}\cdot\mathbf{S} + \mathbf{S_1}\cdot\bar{\bar{\mathbf{D}}}\cdot\mathbf{S_2} \quad (2)$$

where $\bar{\bar{\mathbf{D}}}$ is commonly called the zero-field splitting (ZFS) tensor. The ZFS tensor is comprised of two components, $\bar{\bar{\mathbf{D}}} = \bar{\bar{\mathbf{D}}}_{ss} + \bar{\bar{\mathbf{D}}}_{so}$. $\bar{\bar{\mathbf{D}}}_{ss}$, and arises via the magnetic, through space, dipole−dipole interaction of the two spin centers of the triplet state; $\bar{\bar{\mathbf{D}}}_{so}$ is a through bond, spin−orbit-coupling-derived spin−spin interaction (anisotropic exchange interaction). $\bar{\bar{\mathbf{D}}}_{so}$ is thus $\xi^2\mathbf{\Lambda}$, where ξ is the spin−orbit coupling constant for the molecule, and $\mathbf{\Lambda}$ is the matrix containing elements connecting ground and excited states via the orbital angular momentum operator. In most cases concerning triplet excited states in organic species, the $\bar{\bar{\mathbf{D}}}_{so}$ contribution is negligible, and the resulting triplet EPR spectrum may thus be interpreted using the magnetic dipole−dipole contribution only. Recasting eq 2 in terms of two independent parameters D and E gives rise to the familiar phenomenological spin Hamiltonian,

$$\begin{aligned} H &= \beta_e \mathbf{B}\cdot\bar{\bar{\mathbf{g}}}\cdot\vec{\mathbf{S}} + \mathbf{S_1}\cdot\bar{\bar{\mathbf{J}}}\cdot\mathbf{S_2} \approx \beta_e \mathbf{B}\cdot\bar{\bar{\mathbf{g}}}\cdot\mathbf{S} + \mathbf{S}\cdot\bar{\bar{\mathbf{D}}}_{ss}\cdot\mathbf{S} \\ &= \beta_e \mathbf{B}\cdot\bar{\bar{\mathbf{g}}}\cdot S - (D_{xx}S_x^2 + D_{yy}S_y^2 + D_{zz}S_z^2) \\ &= \beta_e \mathbf{B}\cdot\bar{\bar{\mathbf{g}}}\cdot\mathbf{S} + D(S_z^2 - {}^1/_3 S^2) + E(S_x^2 - S_y^2) \end{aligned} \quad (3)$$

where $-D_{ii}$ ($i = x, y, z$) are the energy eigenvalues of the electron−electron spin interaction; the magnitudes of the zero-field splitting parameters D and E are related to the overall spatial extent, and degree of in-plane asymmetry, respectively, of the of the triplet spin distribution according to the following equations:

$$D = \frac{3}{4}\left(\frac{\mu_o}{4\pi}\right)(g_e\beta_e)^2\left\langle\frac{r^2 - 3z^2}{r^5}\right\rangle = \frac{3}{4}\left(\frac{\mu_o}{4\pi}\right)\frac{(g_e\beta_e)^2}{r^3}\langle 1 - 3\cos^2\theta\rangle \quad (4)$$

$$E = \frac{3}{4}\left(\frac{\mu_o}{4\pi}\right)(g_e\beta_e)^2\left\langle\frac{(y^2 - x^2)}{r^5}\right\rangle \quad (5)$$

Here r is the triplet wave function interelectron distance, x, y, and z are the Cartesian displacements between spin centers projected onto the principal axis system of the molecule, and θ is the polar angle describing the relative orientation of the dipoles. The essential features relating D and electronic structure can be qualitatively seen from the $\langle r^2 - 3z^2\rangle$ term. The expression $\langle r^2 - 3z^2\rangle$ or $\langle x^2 + y^2 - 2z^2\rangle$ is positive ($D > 0$) for an oblate distribution of spin, as one would expect for a planar aromatic molecule, and negative ($D < 0$) for a prolate spin distribution, corresponding to the case often encountered for linear molecules. Expressing eq 4 in terms of the polar angle θ, the extremum at $\theta = \pi/2$ ($D > 0$) corresponds to a parallel, side-by-side triplet spin alignment, while that at $\theta = 0$ ($D < 0$) corresponds to a head-to-tail spin alignment. Thus, at a fixed center-to-center distance r, the limiting cases give $D(\theta = 0) = -2D(\theta = \pi/2)$. For planar aromatic molecules where the spin distribution is oblate (disklike), $\langle z\rangle \ll \langle r\rangle$, and hence, the expression for D reduces to

$$D \cong \frac{3}{4}\left(\frac{\mu_o}{4\pi}\right)(g_e\beta_e)^2\frac{1}{\langle r^3\rangle} \quad (6)$$

congruently, for prolate (tubular) spin distributions

$$D \cong -\frac{3}{4}\left(\frac{\mu_o}{4\pi}\right)(g_e\beta_e)^2\frac{2}{\langle r^3\rangle} \quad (7)$$

Clearly, from eqs 6 and 7, one may extract information regarding the spatial extent of the triplet excitation from the magnitude of the D ZFS parameter. In the point dipole approximation, the spatial extent may be directly determined using the following expressions:

$$D = 1.304\left(\frac{1 - 3\cos^2\theta}{r^3}\right)\text{Å}^3\ \text{cm}^{-1} \quad \text{or}$$

$$r = \left[1.304\left(\frac{1 - 3\cos^2\theta}{D}\right)\right]^{1/3}\text{Å}\ \text{cm}^{-1/3} \quad (8)$$

Equation 8 historically has been used to estimate the extent of triplet species in π-conjugated oligomeric and polymeric materials. Problems arising from using the dipole approximation stem from the extent of spin−orbit coupling and the nature of conjugation; hence, application of eq 8 to determine the expectation value of the interelectron distance in large conjugated systems such as those discussed herein provides only an approximation for this quantity.

As stated previously, the $|E|$ ZFS parameter measures deviations from axial symmetry. The quotient $3|E|/|D|$ lies in the range $0 \le 3|E|/|D| \le 1$; here, the two extremes represent axial symmetry ($|E| = 0$) and orthorhombic symmetry ($3|E|/|D| = 1$).[30,36,44] Molecules which possess a 3-fold or higher rotational axis of symmetry, typically have vanishingly small E values.

For randomly oriented triplet species, the EPR powder spectrum in the $|\Delta M_s| = 1$ region is in general composed of six resonances, two for each canonical orientation of the magnetic field, when the external applied field is parallel to a principal molecular axis. For $|D| \ll h\nu$, the $|\Delta M_s| = 1$ spectrum yields the ZFS parameters directly via the following expressions:

$$\begin{aligned} |D| &= \frac{(g\beta_e)^2}{4h\nu}(B_{lZ}^2 - B_{hZ}^2) \\ |D + 3E| &= \frac{(g\beta_e)^2}{2h\nu}(B_{lX}^2 - B_{hX}^2) \\ |D - 3E| &= \frac{(g\beta_e)^2}{2h\nu}(B_{lY}^2 - B_{hY}^2) \end{aligned} \quad (9)$$

where B_{li} and B_{hi} ($i = X, Y, Z$) are the low-field and high-field canonical transitions, respectively. Thus, for randomly oriented triplet state molecules, the EPR spectrum results in six observable lines or turning points in the first derivative spectrum. Assuming that D is positive and $D \ll h\nu$ as is commonly observed for planar aromatics, and $E > 0$ (an arbitrary assignment), the $|0\rangle \leftrightarrow |+1\rangle$ transition has Z, X, and Y components at field positions displaced approximately from that of free electron ($h\nu/g_e\beta_e$) by $-D$, $+(D + 3E)/2$, and $+(D - 3E)/2$, corresponding to Z_I, X_I, and Y_I field positions, respectively. Likewise, the $|0\rangle \leftrightarrow |-1\rangle$ transition has lines at field positions displaced from g_e by $+D$, $-(D + 3E)/2$, and $-(D - 3E)/2$ that are defined as the Z_{II}, X_{II}, and Y_{II} transitions, respectively, following the convention of Thurnauer.[30,33,36,46] Thus, from the resulting randomly oriented spectrum, ZFS parameters are readily extractable, with the separations in field units between pairs of transitions given as: $\Delta B_z = 2|D|$, $\Delta B_x = |D| + 3|E|$, and $\Delta B_y = |D| - 3|E|$. Because of the arbitrary assignment of the canonical X and Y directions, previous studies have adopted the convention of Thunauer.[30,33,36,46] In this study, we have assigned the X and Y canonical transitions in accordance to the spin redistribution that occurs along the long axis of

conjugation (vide infra). This is in accordance with corresponding optical spectroscopy, where this axis has been defined as the *x*-direction.[27,29−32]

Spin state dynamics can be inferred from the EPR excited triplet spectrum under steady-state illumination conditions.[30,36,46] As entry into the lowest triplet state is governed primarily by spin−orbit coupling, at temperatures (typically in the vicinity of liquid helium) where the $S_0 \leftarrow T_1$ lifetime is short compared to the spin lattice relaxation time between two spin state sublevels (T_1), a non-Boltzmann occupation (electron spin polarization or, more appropriately, electron spin alignment) of the triplet manifold results. Hence, some transitions will be emissive (**e**) in nature while those that are absorptive (**a**) will be enhanced. The resulting polarization pattern of absorptions and emissions under conditions of steady-state illumination can thus be used to ascertain information concerning intersystem crossing (ISC), spin dynamics, and relaxation.[30,36,46]

C. Photoexcited Triplet State EPR Spectral Data. Figure 3 shows the photoexcited triplet state EPR spectra of the compounds **1**−**4** displayed in Figure 1 in the $|\Delta M_s| = 1$ region; these spectra were obtained at 4 K in a glassy matrix of 10:1 toluene:pyridine. All compounds examined in this study possess g values of 2.003 ± 0.002, and demonstrate a $|\Delta M_s| = 2$ transition in the vicinity of 160 mT ($g \sim 4$), indicating that the spin system in question is a $S = 1$ triplet state with no significant orbital angular momentum contribution. The $|\Delta M_s| = 2$ (half-field) transition for compound **2** is shown as an inset in Figure 3; note that the transition is essentially a symmetric Gaussian resonance with an ∼1.5 mT line width. Comparable non-Boltzmann spin alignment within the lowest energy electronically excited triplet state is seen in compounds **3** and **4**.

Figure 4 displays analogous photoexcited triplet state EPR spectral data for electronically symmetric compounds for **5**, **6**, and **7** (Figure 1). Monomeric compounds **5** and **6** feature 5,-15-bis[4-dimethylamino(phenyl)]ethynyl and 5,15-bis[4-nitro-(phenyl)]ethynyl substitution patterns, respectively; note that these species exhibit markedly similar photoexcited EPR spectra with respect to that obtained for 5-[4′-dimethylamino(phenyl)]-ethynyl-15-[4″-nitrophenyl(phenyl)]ethynyl-substituted **1** (Figures 3 and 4), indicating that electronic asymmetry exerts little influence over the nature of the non-Boltzmann spin alignment in these compounds. Similarly, compound **7**, a *meso*-to-*meso* ethyne-linked tris[(porphinato)zinc(II)] species, bearing terminal [4-di-
methylamino(phenyl)]ethynyl units, manifests a X-band EPR spectrum (Figure 4) of its optically pumped low-lying triplet excited state that is closely related to analogous data obtained for push−pull conjugated porphyrin oligomers **3** and **4** (Figure 3). Interestingly, temperature-dependent electronically excited triplet EPR spectra of compound **7** demonstrate that spin polarization is maintained up to 50 K; similar data reveal that all these arylethynyl-derivatized porphyrin oligomers (**2**, **3**, and **4**) maintain spin polarization up to at least this temperature. Congruently, temperature-dependent electron spin polarization experiments show that electronically symmetric *meso*-ethynyl-linked porphyrin oligomeric systems maintain spin polarization up through the glass transition temperature (∼120 K) with little change in the polarization ratios of the canonical transitions.[36] These data point to the fact that over these wide temperature ranges, the spin lattice relaxation time exceeds greatly the triplet state lifetime (vide infra). Consequently, huge spin polarization enhancements are observed in the **1**−**7** EPR powder spectra of the randomly oriented electronically excited triplet states of these species.

The polarization profile obtained from the $|\Delta M_s| = 1$ region of the triplet EPR spectrum provides information regarding the selective entry into the triplet manifold from the first excited singlet state.[46] The polarization profile for compounds **1** and **5**−**7** (Figures 3 and 4) show clearly an **aaa**−**eee** pattern (where **a** and **e** denote respectively transitions enhanced in absorption and emission), indicative of selective intersystem crossing from the excited singlet state (S_1) into the $|T_z\rangle$ spin sublevel of the T_1 state. This polarization pattern is the same as that seen in monomeric (porphinato)zinc(II) (PZn) species.[36] Note that the spectra obtained for conjugated oligomers **2**, **3**, and **4** evince overlapping low- and high-field *Z* and *X* canonical transitions that are respectively enhanced in absorption (**a**) and emission (**e**); straightforward spectral deconvolution and line width analyses support clearly this contention. In the monomeric compounds **1**, **5**, and **6** where the *Z* and *X* transitions are well separated, the *Z* and *X* absorption line widths lie in the 20.5−23.5 G (2.05−2.35 mT) range, while oligomers **2**−**4** and **7** manifest line widths for these transitions that span 32.0−35.2 G (3.2−3.52 mT). This observed line width increase of the overlapping *Z* and *X* transitions in the conjugated oligomers relative to monomeric species **1**, **5**, and **6** corresponds to a field separation of ∼2 mT between the *Z* and *X* canonical transitions. It is conspicuous that there is no evidence consistent with any reversal of the polarization pattern that would signal significant electronic perturbation to the electronically excited triplet wave functions of compounds **1**−**7** relative to those probed previously in analogous conjugated porphyrin oligomers lacking terminal arylethynyl groups.[30,33,36]

In contrast to similar experiments that probe the nature of the spin distribution in the low-lying electronically excited triplet state of poly(*p*-phenylvinylenes[47,48] and poly(alkythiophenes),[48,49] no EPR spectroscopic signatures of radical (polaron) species were observed in any of the spectra obtained for **1**−**7** under CW photoexcitation conditions. These results attest to the established photostability of these compounds at cryogenic temperatures; in further contrast to these experiments that probe the T_1 states of these classes of technologically important conjugated materials,[47−49] it is noteworthy that no measurable concentration of spin-$^1/_2$ species has ever been observed following prolonged electronic excitation of **1**−**7** and highly related species under a wide range of experimental conditions.[24,28−31,33,36,38]

The ZFS parameters, evaluated using eq 9 for compounds **1**−**7** as well as several monomeric PZn species, are recorded in Table 1. As is evident, the $|D|$ ZFS parameter for compounds **1**−**4** changes by ≤2% over the series for $n = 1-4$ where n is the number of oligomeric porphyrin units in the oligomer. Because the Zn-to-C_β distance is ∼0.43 nm in a typical (porphinato)zinc(II) monomer, these tabulated $|D|$ values, coupled with the observed polarization patterns (vide supra), demonstrate that triplet excitation is confined to spatial dimensions that do not exceed that of a single monomeric porphyrin unit and its pendant, cylindrically π symmetric, ethynyl substituents.

Prior to discussing in detail the T_1 state spatial extent in these species, the rhombicity factors, $3|E|/|D|$, for compounds **1**−**7** deserve some comment, as this quantity provides added insight into the nature of the T_1 state electron density distribution. Although the magnitude of the spatial extent, estimated from the $|D|$ ZFS parameter, is invariant in this series of conjugated oligomers, analysis of the $|E|$ ZFS parameter does reveal more subtle perturbations to the triplet spin geometry. As is clearly demonstrated in electronically symmetric *meso*-to-*meso* ethyne-

TABLE 1: Observed Zero-Field Splitting Parameters for Compounds 1−7, and Benchmark Monomeric and Ethyne-Bridged Bis(porphyrin) Structures[a,b]

compound	T/K	P/μW	$\lvert D\rvert$/cm^{-1}	$\lvert E\rvert$/cm^{-1}	rhombicity $3\lvert E\rvert/\lvert D\rvert$	$\langle r\rangle$/nm[c]	ref
DPPZn	4	2	0.0326	0.0094	0.865	0.342	36
TPPZn	4	2	0.0306	0.0095	0.931	0.350	36
5-E-DPPZn	4	2	0.0315	0.0048	0.457	0.346	36
5,15-DE-DPPZn	4	2	0.0301	0.0053	0.528	0.352	36
2A	4	2	0.0319	0.0106	1	0.43	30, 36
1	4	10	0.0301	0.0077	0.769	0.352	this work
2	4	10	0.0303	>0.009	>0.9	0.441	this work
3	4	10	0.0300	>0.009	>0.9	0.443	this work
4	4	2	0.0301	>0.009	>0.9	0.42	this work
5	4	10	0.0304	0.0079	0.782	0.351	this work
6	10	10	0.0304	0.0080	0.786	0.351	this work
7	4	10	0.0298	0.0090	0.901	0.444	this work

[a] Solvent: 10:1 toluene:pyridine. Modulation amplitude: 2 mT at 100 kHz. [b] ZFS values ± 0.0002. [c] Values determined using point-dipole approximation.

linked porphyrin oligomers, while the spatial extent of triplet excitation does not scale with molecular dimension and thus remains strongly localized, a spin redistribution accompanies the augmentation of conjugation length.[30,33,36]

It has been previously demonstrated for closed-shell PZn-based multichromophore arrays, in which ethyne or butadiyne units bridge the constituent macrocycles at their respective *meso*-carbon positions, that the triplet state electronic structure is perturbed with respect to that observed for analogous β-to-β and *meso*-to-β-linked multiporphyrin compounds.[36] The photoexcited triplet states of *meso*-to-*meso* ethyne- and butadiyne-bridged PZn arrays manifest a reorientation of the axis of greatest dipolar coupling from Z (perpendicular to the porphyrin plane) to X (along the highly conjugated *meso*-to-*meso* bridge); this redistribution occurs concomitant with a decrease in the $\lvert D\rvert$ ZFS parameter.[30,36] This oblate-to-prolate spin transition observed for **2A** (and its bis[(porphinato)zinc(II)] analogue that features a *meso*-to-*meso* butadiyne linker) in the lowest photoexcited triplet state correlates with the enhanced chromophore−chromophore coupling made possible by this linkage topology relative to that determined for corresponding bis(chromophoric) complexes that possessed *meso*-to-β or β-to-β bridging motifs.[29,31,32,36]

As emphasized above, in the limit of $3\lvert E\rvert/\lvert D\rvert = 1$, the spin distribution assumes orthorhombic symmetry; in such a case the *Z* and *X* canonical transitions overlap and the corresponding low and high-field *Y* transitions become coincident. As observed previously for related PZn structures at low temperature,[30,36] the *Y* transitions highlighted in the EPR spectra of Figures 3 and 4 carry spin polarization such that the low-field transition is enhanced in absorption while the high-field transition is enhanced in emission. When these spin polarized transitions overlap in the orthorhombic limit, they result in essentially zero signal in the photoexcited EPR spectrum. As exemplified in compounds **2**−**4** (Figure 3 arrows), the *X* transitions are either coincident with, or nearly crossing over, what were the *Z* transitions, resulting in $3\lvert E\rvert/\lvert D\rvert$ values that approach unity (Table 1, vide infra). Furthermore, in **2**−**4**, it is clearly evident that the Y_I and Y_{II} transitions overlap extensively at $g = 2.00$; because the former transition is absorptive and the latter is emissive, reduced signal intensity is observed in this spectral region.

As is evident from Table 1 data, the simple PZn monomers such as **DPPZn** and **TPPZn** (Figure 1) have $(3\lvert E\rvert/\lvert D\rvert)$ ratios of 0.931 and 0.865 respectively,[36] evincing the orthorhombic symmetry expected for circular absorbers with essentially degenerate x- and y-polarized excited states.[28,31,36,50] When cylindrically π symmetric ethynyl groups are fused to the macrocycle *meso* position in PZn monomers, substantial energetic splitting between the *x*- and *y*-polarized transitions are manifest;[24,27,31,32,38,39] These energetic differences are evident in the photoexcited triplet EPR spectra. Note that the *E* value determined for **5-E-DPPZn**, which reflects the degree of in plane symmetry of its corresponding electronically excited triplet state, evolves substantially toward the axial limit ($3\lvert E\rvert/\lvert D\rvert = 0.457$) with respect to **DPPZn** and **TPPZn**; interestingly, additional augmentation of conjugation along the axis defined by **5-E-DPPZn**'s ethynyl group results in a **5,15-DE-DPPZn** T_1 state EPR spectrum in which the *E* value is further enhanced ($3\lvert E\rvert/\lvert D\rvert = 0.527$), indicating a triplet state slightly more orthorhombic in nature.[30,36] Compound **1** (Figures 1 and 3), which features expanded conjugation along its molecular *x*-axis relative to **5,15-DE-DPPZn**, has been established to possess a singly degenerate S_1 state in which the energetic separation of *x*- and *y*-polarized states are enhanced with respect to both **5-E-DPPZn** and **5,15-DE-DPPZn**;[24,38,39,51,52] this compound manifests a $3\lvert E\rvert/\lvert D\rvert$ value of 0.769 (Table 1).

The axis of the largest dipolar interaction is traditionally labeled the molecular *z*-axis; for monomeric porphyrinoid compounds, it is firmly established that this axis lies perpendicular to the porphyrin plane. Conventional triplet spin distributions in such systems are consequently oblate in nature (a classic side-by-side dipole arrangement, $\theta = 90°$) with D positive (eq 6). With increasing conjugation perpendicular to the *z*-axis, the triplet spins are free to evolve into a more prolate spin distribution (a head-to-tail dipole arrangement, $\theta = 0°$) resulting in *D* becoming negative (eq 7). An oblate-to-prolate transition may be monitored by observing the evolution of $\lvert E\rvert$ as conjugation is elaborated along the axis perpendicular to the molecular *z*-axis. In such a case, $\lvert E\rvert$ should tend toward the orthorhombic limit of the rhombicity ($3\lvert E\rvert/\lvert D\rvert = 1$); beyond this critical limit, a new axis of largest dipolar interaction emerges, namely the axis of conjugation.

Previous analyses of the evolution of T_1 state spin distribution in electronically symmetric *meso*-to-*meso* ethyne-(**2A, 3A, 5A**; Figure 1) and butadiyne-bridged porphyrin oligomers,[30,33,36] strictly defined a prolate distribution for cases where the computed asymmetry parameter ($3\lvert E\rvert/\lvert D\rvert$) evolved with increasing conjugation to a value of 1 when an oblate spin distribution was assumed ($\theta = 90°$); at this limit, by definition, a head-to-tail arrangement ($\theta = 0°$) of triplet spins must be assumed (see for example EPR data obtained for compound **2A**, Table 1). This redistribution of spin density in the photoexcited triplet state causes the axis of largest dipolar coupling to align along *X* (the axis lying in plane and along the axis of conjugation). In contrast to the case established for these electronically symmetric

highly conjugated PZn oligomers, by this criterion the orthorhombic limit is not reached in compounds **1**−**7**; note, however, that the $|E|$ ZFS parameter is observed to increase monotonically toward that limit: **5-E-PZn** < **5,15-DE-PZn** < **1** < **2** < **3**, **4**, and **7** (Table 1 and Figure 1). This observed evolution of the asymmetry parameter ($3|E|/|D|$) with augmented conjugation is consistent with a progressing rotation of the magnetic principal axis system that causes the direction of largest dipolar interaction to evolve along the vector defined by the conjugated ethyne moiety.[30] Changes in the magnetic anisotropy are manifested in the photoexcited triplet states of compounds **5-E-DPPZn**, **5,15-DE-DPPZn**, **1**, **2**, **3**, **4**, and **7** are thus seen to mirror the changes evinced in the excited-state polarization of the S_1 states of these species, signaling that the magnetic and optical principal axis systems migrate with increasing conjugation toward an identical reference frame.[30] This evolution of the triplet spin distribution in ethyne- and butadiyne-linked oligomeric porphyrin structures appears unique among the π-conjugated oligomeric and polymeric materials thus far investigated.

Estimation of the spatial extent of the T_1 state wave function depends critically on whether an oblate or prolate distribution is assumed. Further, using the point-dipole approximation (eq 8), a computed T_1-state inter-electron distance increases concomitant with the oblate-to-prolate spin redistribution. In this regard, two points are worth emphasizing: (i) given the head-to-tail dipole orientation of the prolate spin dipolar interaction and the potentially complex nature of the T_1 wave function, such calculated inter-electron separations should only be viewed as very rough approximations and, (ii) importantly, regardless which limiting model is most appropriate for estimating T_1 state inter-electron distances for these oligomers, the distances calculated in either the oblate or prolate spin distribution limits do not exceed the spatial dimension spanned by a single PZn unit and its *meso*-pendant ethynyl group(s) in oligomers **2**−**4** and **7**.

In an attempt to make meaningful comparisons between these conjugated porphyrin systems and similar literature data obtained for other classes of conjugated oligomers (vide infra), as the computed values of the asymmetry parameter for compounds **2**, **3**, **4**, and **7** ($3|E|/|D| > 0.9$) signal that the spin distribution is approaching the orthorhombic limit, we assume in these cases that a head-to-tail dipole spin arrangement ($\theta = 0°$, eq 7), models more effectively the T_1 state wave function electron density distribution. For systems studied where the values of $3|E|/|D| \leq 0.9$, we take the axis of largest dipolar coupling to be along the standard Z (perpendicular to porphyrin plane) for such triplet-state inter-electron distance calculations. For electronically asymmetric *meso*-to-*meso* ethyne-bridged porphyrinic oligomers **2**−**4** and **7**, the T_1 state spatial extent is found to be uniformly 4.4 Å (0.44 nm), contrasting starkly the electronic structures of their corresponding S_1 states. Note in this latter regard that the donor-to-acceptor distance in oligomer **4** exceeds 50 Å. Recent studies that probe the radical monocationic (hole polaron) state of a linear, electronically symmetric pentameric porphyrin oligomer having identical linkage topology with respect to **2**−**4** but lacking the electron releasing and donating end-capping groups, show evidence of rapid dynamics (on the time scale of electron−nuclear hyperfine couplings) of the polaron over the linear dimension of the molecule,[53] further underscoring the apparently special electronic feature of the low-lying triplet excited state within this class of conjugated structures.

With respect to the issue of T_1 state wave function spatial localization, previous EPR investigations of *meso*-to-*meso* ethyne-linked porphyrin species, where electronic asymmetry was introduced via the juxtaposition of PZn and simple porphyrin macrocycle (PH_2) units, also evinced similar triplet excitation localization.[30] Electronic asymmetry introduced via peripheral arylethynyl-linked electron-donating and electron-releasing groups (Figure 1) gives rise to qualitatively similar T_1 state EPR spectra with respect to that observed for conjugated porphyrin oligomers that feature such PZn-to-PH_2 electronic structural heterogeneity, as well as quantitatively similar evaluated EPR D values. Likewise, transient and resonance Raman spectroscopic studies of the Cu(II) analogue of compound **1** demonstrate that the triplet manifold possesses many features in common with the trip-doublet and trip-quartet ($^2T-^4T$) states of simple (5,10,15,20-tetraphenylporphinato)copper(II) (**TPPCu**) species; most importantly, neither Raman nor pump−probe optical spectroscopy indicated that the long-lived triplet states of the Cu(II) analogue of compound **1** featured either measurable charge-transfer interactions, involving the porphyrin and peripheral arylethynyl groups, or T_1 state excitation delocalization that exceeded that of the **TPPCu** benchmark.[38] Finally, it is clear from the tabulated $|D|$ and $|E|$ ZFS values (Table 1) that electronically asymmetric **1** and electronically symmetric **5** and **6** manifest no measurable differences with respect to these spectroscopically evaluated parameters; similarly, no change in ZFS parameters is noted between the oligomers **3** and **7**, despite their markedly different ground (S_0) and singlet-excited state electronic structures, further solidifying the conclusion that the spatial extent of the triplet spin distribution within this family of conjugated oligomers is *unaffected* by the arylethynyl pendant electron-withdrawing or -releasing groups.

D. Electron Spin−Spin and Spin−Lattice Relaxation of the $S = 1$ State. In addition to using spectrally evaluated parameters to obtain insight regarding the nature of the photoexcited triplet state, EPR spectroscopy can also be used to gather information regarding spin dynamics, which is embodied in the spin−spin and spin−lattice relaxation time constants. In this regard, we have determined the spin−spin and spin−lattice relaxation times for the triplet exciton in compounds **5** and **7** over the 4−30 K temperature range. As relaxation of the triplet exciton is governed primarily by modulation of the ZFS interaction, it is hypothesized that triplet exciton migration should result in enhanced spin−lattice relaxation where there is monomeric unit-to-unit disorder,[54] resulting in a decrease in the spin−lattice relaxation time with increasing conjugation length. A corresponding absence of spin−lattice relaxation scaling with conjugation length would suggest that the triplet exciton is confined to one monomeric unit.

The signal strength of the inhomogeneously broadened Z_I and Z_{II} canonical transitions were assessed as a function of the incident microwave power under steady-state optical pumping conditions (Figure 5). Both the spin−spin (T_2) and spin−lattice (T_1) relaxation times were determined from plots of the signal strength vs the square root of the microwave power using the theory of Wheeler et al.[41] The relaxation times were ascertained at 4, 10, 20, and 30 K. At 4 K, the T_2 relaxation times for compounds **5** and **7** were determined to be $(3.33 \pm 0.9) \times 10^{-8}$ and $(2.3 \pm 0.17) \times 10^{-8}$ s, respectively, while the corresponding T_1 relaxation times were evaluated to be $(5.6 \pm 0.6) \times 10^{-3}$ and $(5.4 \pm 1.3) \times 10^{-3}$ s. At 30 K, the T_2 relaxation times for compounds **5** and **7** remain statistically unchanged at $(5.8 \pm 6.1) \times 10^{-8}$ and $(5.6 \pm 2.9) \times 10^{-8}$ s respectively, while the analogous **5** and **7** T_1 times decrease modestly to $(1.4 \pm 1.3) \times 10^{-3}$ and $(0.79 \pm 0.38) \times 10^{-3}$ s, respectively. Given that the

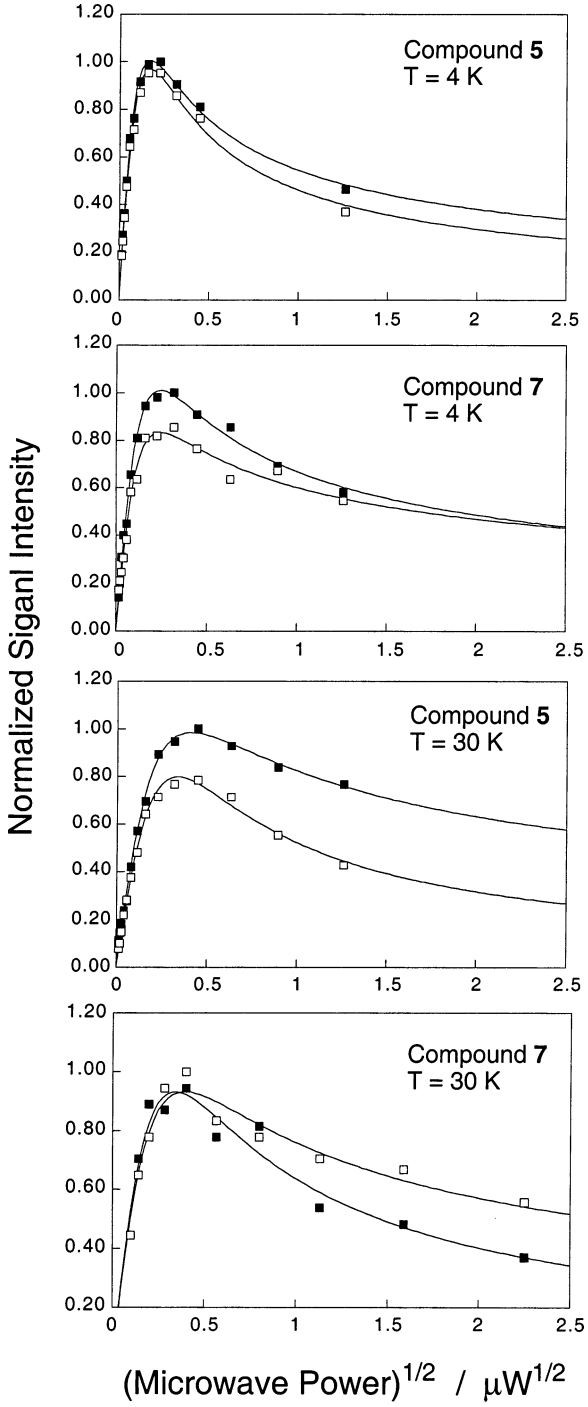

Figure 5. Signal intensity of the low-field (Z_I) and high-field (Z_{II}) canonical transitions as a function of the square root of the microwave power for compounds **5** and **7** at 4 and 30 K. Solid squares: low-field (Z_I) canonical transition; open squares: high-field (Z_{II}) canonical transitions. The solid lines are a fit to $Y' = \sqrt{P}/(1 + P/P_{1/2})^{b/2}$, where P is the incident microwave power, $P_{1/2}$ is the saturation parameter, and b is a measure of spectral inhomogeneity.

lifetime of the lowest energy electronically excited triplet state is estimated to be on the order of 100 μs at 298 K from pump−probe transient optical experiments that interrogate the $T_1 \rightarrow T_n$ transitions of these systems (data not shown),[30,36] it can only be concluded that these electronically excited triplet lifetimes would be somewhat longer at lower temperatures; thus, the spin−lattice relaxation times are more than an order of magnitude greater than the T_1 lifetimes, consistent with the observed maintenance of electron spin polarization over substantial temperature ranges in this class of conjugated oligomers.[36] While the T_2 and T_1 relaxation times do not statistically change with conjugation length, and T_2 is essentially invariant with respect to temperature, the spin−lattice relaxation times on the other hand, show a monotonic decrease with increasing temperature that is roughly determined by a power law with an exponent of ~2. This is consistent with previous data obtained for an extensive body of ethyne- and butadiyne-bridge porphyrin oligomers[36] and experiments carried out by Friedrich that examined triplet spin lattice relaxation of aromatic chromophores in glassy matrices.[55−57] Last, it is observed that the T_1 relaxation time is not significantly different in the tris[(porphinato)zinc-(II)] species **7** relative to monomeric compound **5**, consistent with the hypothesis that these species possess qualitatively similar electronically excited triplet-state wave functions.

IV. Concluding Remarks and the Universality of Localized Triplet Excitations in π-Conjugated Materials

This work shows that *meso*-to-*meso* ethyne-linked porphyrin oligomers that possess electronic asymmetry deriving from conjugation of electron releasing and electron withdrawing moieties to their respective terminal *meso*-carbon positions do not manifest augmented T_1 state interelectron distances relative to their corresponding parent, conjugated oligoporphyryl benchmarks. In all the conjugated (porphinato)zinc(II) oligomers studied, the triplet excitation yielded ZFS parameters indicative of a strongly confined triplet excitation, the extent of which does not significantly exceed a single monomeric porphyrin unit and its *meso*-pendant ethynyl moieties (~0.42 nm). Data obtained from progressive microwave saturation experiments yielding spin−spin and spin−lattice relaxation times support the conclusion that triplet state excitation is confined over this spatial dimension. That the spatial extent of the triplet spin distribution varies by less that 0.02 nm in compounds **2**−**4** and **7** is particularly striking, given that the linear dimensions of these highly conjugated structures range from 3.4 to 5.6 nm.

Seminal studies of the photoexcitations in polyalkylthiophenes and polyphenylenevinylenes using ODMR showed the presence of triplet states yielding ZFS parameters suggestive of localized excitations.[47−49] Given (i) the enhanced electron−lattice interactions demonstrated in polyalkylthiophenes and polyphenylenevinylenes relative to the π-conjugated oligomers investigated in this study[16] and (ii) the fact that the magnitude of porphyrin inner sphere reorganization energy is dramatically reduced relative to that determined for phenylenes and thiophenes made perhaps controversial, when first reported,[36] the observation that ethyne- and butadiyne-bridged (porphinato)zinc(II) oligomers that feature *meso*-to-*meso*, *meso*-to-β, and β-to-β linkage topologies between adjacent macrocycles possess highly localized excited triplet state wave functions was controversial. This finding now appears to be a completely general result; moderate degrees of electronic asymmetry, whether introduced via a combination of potentiometric and excited-state polarization modulation of a particular monomeric porphyrinic building block[30] or by introduction of potent electron donating or releasing moieties to the termini of such conjugated oligomers, have been seen to have no impact on the magnitude of the maximal T_1 state interaction distance (~0.44 nm) in these systems. In this regard, it is worth noting that time-resolved microwave conductivity measurements have been carried out on a small subset of the aforementioned conjugated oligomeric porphyrin species that features a *meso*-to-*meso* butadiynyl linkage topology; these microwave conductivity measurements determine excess polarizability volumes of < 50 Å^3 for the

TABLE 2: Spatial Extent of Triplet Wave Functions of a Wide Range of Conjugated Materials Measured by the $|D|$ ZFS Parameter and Analyzed within the Context of the Point−Dipole Approximation

material[a]	$\|D\|/cm^{-1}$	$\|E\|/cm^{-1}$	$3\|E\|/\|D\|$	$r\ (\theta = 90°)$ $(D > 0)$[e]	$r\ (\theta = 0°)$ $(D < 0)$[e]	technique[b]	ref
			Porphyrin Oligomers				
meso−*meso* yne dimer	0.0319	0.0106	0.997	(3.44)	4.34	EPR	33, 36
meso−*meso* yne trimer	0.0303	0.0101	1.000	(3.50)	4.41	EPR	33, 36
meso−*meso* butadiyne dimer	0.0447	0.0097	0.651	3.08	(3.88)	EPR	33, 36
meso−*meso* butadiyne trimer	0.0408	0.0089	0.654	3.17	(4.00)	EPR	63
meso−*meso* yne T-shaped trimer	0.0297	0.0093	0.939	(3.53)	4.44	EPR	33
meso−*meso* yne pentamer	0.0286	0.0086	0.902	(3.57)	4.50	EPR	33
DPA (compound **1**)	0.0301	0.0077	0.769	(3.51)	4.42	EPR	this work
DPPA (compound **2**)	0.0303	>0.009	>0.9	3.50	(4.41)	EPR	this work
DPPPA (compound **3**)	0.0300	>0.009	>0.9	3.51	(4.43)	EPR	this work
DPPPPA (compound **4**)	0.0301	>0.009	>0.9	3.51	(4.42)	EPR	this work
yPyyPy (butadiyne dimer)				3.36	4.17	TRMC	35
$(yPy)_5$ (butadiyne pentamer)				3.36	4.17	TRMC	34
			Thiophene Oligomers				
EC2T	0.0972			2.37	(2.99)	EPR	58
EC3T(1)	0.0785	0.0023	0.088	2.55	(3.21)	EPR	58
EC3T(2)	0.0785	0.0074	0.283	2.55	(3.21)	EPR	58
EC4T	0.0682	0.0023	0.101	2.67	(3.37)	EPR	58
EC5T	0.0645	0.0019	0.088	2.72	(3.43)	EPR	58
EC6T	0.0626	0.0019	0.091	2.75	(3.46)	EPR	58
Th3(unsubstituted oligothio)					(3.27)	EPR	61
Th4(unsubstituted oligothio)					(3.36)	EPR	61
Th5(unsubstituted oligothio)					(3.49)	EPR	61
3T1D(1)	0.0813	0.0028	0.103	2.52	(3.18)	EPR	58
3T1D(2)	0.0813	0.007	0.258	2.52	(3.18)	EPR	58
6T2D	0.0644	0.0042	0.196	2.72	(3.43)	EPR	58
8T4D	0.0598	0.0032	0.161	2.79	(3.52)	EPR	58
P3AT	0.0523	0	0.000	(2.92)	3.68	ODMR	49
PT				2.92[c]	3.63[d]	TRMC	62
infinite	0.0444				3.89		58
			Poly(*p*-phenylenes)				
m-LPPP	0.0579	0.0006	0.031	(2.82)	(3.56)	ODMR	12
LOPP7	0.0659	0.0065	0.296	(2.70)	(3.41)	ODMR	12
			Poly(*p*-phenylenevinylenes)				
PPV	0.0542			(2.89)	3.64	ODMR	47
PDHOPV	0.0486	0.0162	1.000	(2.99)	3.77	ODMR	47

[a] Abbreviations and acronyms were chosen to match those used in the original publication. [b] EPR: electron-paramagnetic resonance. TRMC: time-resolved microwave conductivity measurement. ODMR: optically detected magnetic resonance. [c] Using a cubic excess polarizability volume. [d] Using a spherical excess polarizability volume. [e] Parentheses indicates values reported in the reference.

respective electronically excited triplet states of such species,[34,35] consistent with excitation confinement to a single porphyrin unit, complimenting the extensive body of photoexcited EPR spectroscopic and pump−probe transient optical data compiled to date.[30,33,36]

Table 2 summarizes data that assess T_1 state excitation delocalization in conjugated oligomers and polymers obtained by a variety of spectroscopic and experimental techniques that include EPR and optically detected magnetic resonance (ODMR) spectroscopies, and time-resolved microwave conductivity measurements; Figure 6 shows the structures of the conjugated materials relevant to the Table 2 data. It is seen clearly in the Table 2 data that in all cases the spatial extent of the triplet excitation lies in the range 0.25−0.45 nm; note that while in some cases a correlation may exist between conjugation length and the spatial extent of triplet spin distribution, such correlations, if they exist, are weak, and no clear scaling relationship has yet to emerge.

We note in the Table 2 data that evaluating the spatial extent of the T_1 wave function extent using the dipolar interaction of an $S = 1$ spin system (in particular using the $|D|$ ZFS parameter) appears to have generated an inconsistency in the literature when applied to conjugated oligomeric and polymeric systems; this inconsistency derives from the fact that the magnitude of the calculated T_1 state interelectron distance depends sensitively on whether the data were analyzed within the context of an oblate or prolate spin distribution (eq 8, vide supra). In Table 2, the spatial extent of the triplet wave function is evaluated at both the extreme angular values of $\theta = 0°$ and $\theta = 90°$ (eqs 4 and 8) for comparison, regardless of the computational assumptions and values reported in the original literature. Relevant to this discussion, Bennati has argued effectively that while the sign of D is not obtained by the EPR experiment, the observation of E values close to zero for the oligomeric thiophenes (oligomers of obvious axial symmetry) almost preclude a positive value for the D ZFS parameter, thus requiring the data to be analyzed within the context of a prolate spin distribution ($\theta = 0°$, eq 8).[58−60] A vanishing E ZFS in conjugated oligomers or polymers composed of monomeric units that do not possess a 3-fold or higher rotation axis perpendicular to the long axis of conjugation clearly mandates that $D < 0$; hence, eq 8 should be used with an extremum value of $\theta = 0°$ to estimate the spatial extent of the spin distribution.

While Table 2 makes clear the comparisons that are appropriate regarding the magnitudes of the evaluated T_1 state interelectron distances for varying classes of conjugated materials, given the crucial caveat of whether the observed spin distributions are oblate or prolate in nature, it is important to note that in either of these limits, it is unambiguous that the spatial extent of the T_1 state wave function is severely restricted relative to

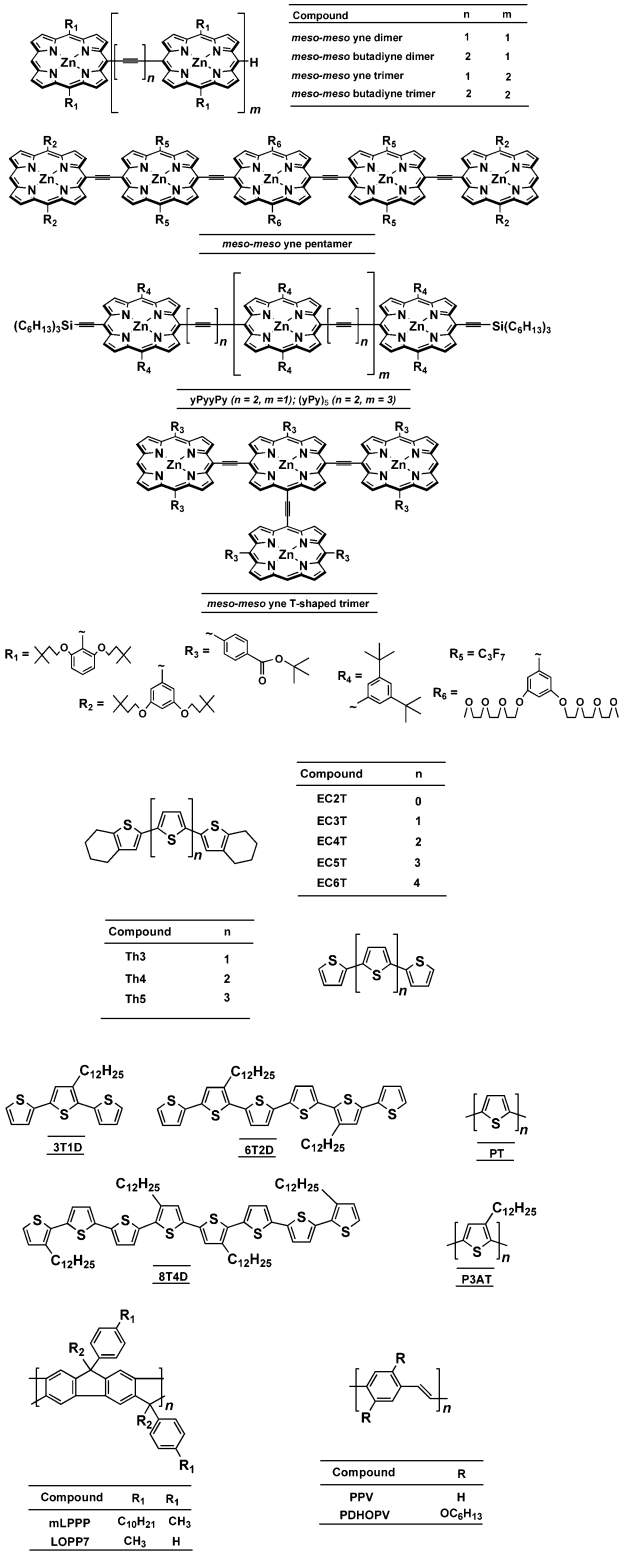

Figure 6. Structures of conjugated oligomers relevant to the Table 2 data. See also Figure 1.

the linear dimension of all the conjugated oligomers and polymers thus far studied. It hence remains to be seen whether the low lying electronically excited T_1 state of any closed-shell diamagnetic conjugated material possesses a spin distribution that exceeds a spatial dimension of 0.5 nm.

Acknowledgment. M.J.T. acknowledges the Division of Chemical Sciences, Office of Basic Energy Research, U.S. DOE (DE-FGO2-02ER15299) for generous financial support.

References and Notes

(1) Robins, L.; Orenstein, J.; Superfine, R. *Phys. Rev. Lett.* **1986**, *56*, 1850.
(2) Lupton, J. M.; Pogantsch, A.; Piok, T.; List, E. J. W.; Patil, S.; Scherf, U. *Phys. Rev. Lett.* **2002**, *89*, 167401.
(3) Wohlgenannt, M.; Jiang, X. M.; Vardeny, Z. V.; Janssen, R. A. *Phys. Rev. Lett.* **2002**, *88*, 197401.
(4) Wohlgenannt, M.; Tandon, K.; Mazumdar, S.; Ramasesha, S.; Vardeny, Z. V. *Nature (London)* **2001**, *409*, 494.
(5) Wilson, J. S.; Dhoot, A. S.; Seeley, A. J. A. B.; Khan, M. S.; Kohler, A.; Friend, R. H. *Nature (London)* **2001**, *413*, 828.
(6) Monkman, A. P.; Burrows, H. D.; Hamblett, I.; Navarathnam, S. *Chem. Phys. Lett.* **2001**, *340*, 467.
(7) Monkman, A. P.; Burrows, H. D.; Hamblett, I.; Navarathnam, S.; Svensson, M.; Anderson, M. R. *J. Chem. Phys.* **2001**, *115*, 9046.
(8) Monkman, A. P.; Burrows, H. D.; Hartwell, L. J.; Horsburgh, L. E.; Hamblett, I.; Navarathnam, S. *Phys. Rev. Lett.* **2001**, *86*, 1358.
(9) Lane, P. A.; Palilis, L. C.; O'Brien, D. F.; Giebeler, C.; Cadby, A. J.; Lidzey, D. G.; Campbell, A. J.; Blau, W.; Bradley, D. D. C. *Phys. Rev. B* **2001**, *63*, 235206.
(10) Romanovskii, Y. V.; Gerhard, A.; Schweitzer, B.; Scherf, U.; Personov, R. I.; Bassler, H. *Phys. Rev. Lett.* **2000**, *84*, 1027.
(11) Shuai, Z.; Beljonne, D.; Silbey, R. J.; Bredas, J. L. *Phys. Rev. Lett.* **2000**, *84*, 131.
(12) List, E. J. W.; Partee, J. S.; J.; Scherf, U.; Mullen, K.; Zojer, E.; Petrtisch, K.; Leising, G.; Graupner, W. *Phys. Rev. B* **2000**, *61*, 10807.
(13) Cao, Y.; Parker, I. D.; Yu, G.; Zhang, C.; Heeger, A. J. *Nature (London)* **1999**, *397*, 44.
(14) Partee, J.; Frankevich, E. L.; Uhlhorn, B.; Shinar, J.; Ding, Y.; Barton, T. J. *Phys. Rev. Lett.* **1999**, *82*, 3673.
(15) Baldo, M. A.; O'Brien, D. F.; Thompson, M. E.; Forrest, S. R. *Phys. Rev. B.* **1999**, *60*, 14422.
(16) Sariciftci, N. S. *Primary photoexcitations in conjugated polymers: Molecular exciton versus semiconductor band model*; World Scientific: River Edge, NJ, 1997.
(17) Qureshi, F. M.; Martin, S. J.; Long, X.; Bradley, D. D. C.; Henari, F. Z.; Blau, W. J.; Smith, E. C.; Wang, C. H.; Kar, A.; K,; Anderson, H. L. *Chem. Phys.* **1998**, *231*, 87.
(18) Wagner, R. W.; Lindsey, J. S.; Seth, J.; Palaniappan, V.; Bocian, D. *J. Am. Chem. Soc.* **1996**, *118*, 3996.
(19) Tour, J. M.; Rawlett, A. M.; Kozaki, M.; Yao, Y.; Jagessar, R. C.; Dirk, S. M.; Price, D. W.; Reed, M. A.; Zhou, C. W.; Chen, J.; Wang, W.; Campbell, I. *Chem.—Eur. J.* **2001**, *7*, 5118.
(20) Wagner, R. W.; Lindsey, J. S. *J. Am. Chem. Soc.* **1994**, *116*, 9759.
(21) Screen, T. E. O.; Thorne, J. R. G.; Denning, R. G.; Bucknall, D. G.; Anderson, H. L. *J. Am. Chem. Soc.* **2002**, *124*, 9712.
(22) Kuebler, S. M.; Denning, R. G.; Anderson, H. L. *J. Am. Chem. Soc.* **2000**, *122*, 339.
(23) Albert, I. D. L.; Marks, T.; Ratner, M. A. *Chem. Mater.* **1998**, *10*, 753.
(24) LeCours, S. M.; Guan, H.-W.; DiMagno, S. G.; Wang, C. H.; Therien, M. J. *J. Am. Chem. Soc.* **1996**, *118*, 1497.
(25) Anderson, H. L.; Martin, S. J.; Bradley, D. D. C. *Angew. Chem., Int. Ed. Engl.* **1994**, *33*, 655.
(26) Suslick, K. S.; Chen, C.-T.; Meredith, G. R.; Cheng, L.-T. *J. Am. Chem. Soc.* **1992**, *114*, 6928.
(27) Lin, V. S.-Y.; DiMagno, S. G.; Therien, M. J. *Science* **1994**, *264*, 1105.
(28) Rubtsov, I. V.; Susumu, K.; Rubtsov, G. I.; Therien, M. J. *J. Am. Chem. Soc.* **2003**, *125*, 2687.
(29) Susumu, K.; Therien, M. J. *J. Am. Chem. Soc.* **2002**, *124*, 8550.
(30) Shediac, R.; Gray, M. H. B.; Karki, L.; Hupp, J. T.; Angiolillo, P. J.; Therien, M. J. *J. Am. Chem. Soc.* **2000**, *122*, 7017.
(31) Kumble, R.; Palese, S.; Lin, V. S.-Y.; Therien, M. J.; Hochstrasser, R. M. *J. Am. Chem. Soc.* **1998**, *120*, 11489.
(32) Lin, V. S.-Y.; Therien, M. J. *Chem.—Eur. J.* **1995**, *1*, 645.
(33) Angiolillo, P. J.; Susumu, K.; Uyeda, H. T.; Lin, V. S.-Y.; Shediac, R.; Therien, M. J. *Synth. Met.* **2001**, *116*, 247.
(34) Piet, J. J.; Taylor, P. N.; Wegewijs, B. R.; Anderson, H. L.; Osuka, A.; Warman, J. M. *J. Phys. Chem. B* **2001**, *105*, 97.
(35) Piet, J. J.; Taylor, P. N.; Anderson, H. L.; Osuka, A.; Warman, J. M. *J. Am. Chem. Soc.* **2000**, *122*, 1749.
(36) Angiolillo, P. J.; Lin, V. S.-Y.; Vanderkooi, J. M.; Therien, M. J. *J. Am. Chem. Soc.* **1995**, *117*, 12514.
(37) Angiolillo, P. J.; Uyeda, H. T.; Therien, M. J. *Bull. Am. Phys. Soc.* **2001**, *46* (1), 763.
(38) LeCours, S. M.; Phillips, C. M.; De Paula, J. C.; Therien, M. J. *J. Am. Chem. Soc.* **1997**, *119*, 12578.
(39) Priyadarshy, S.; Therien, M. J.; Beratan, D. N. *J. Am. Chem. Soc.* **1996**, *118*, 1504.
(40) Wortmann, R.; Uyeda, H. T.; Therien, M. J. Manuscript in preparation.

(41) Wheeler, D. D.; Farach, H. A.; Poole, C. P., Jr.; Creswick, R. J. *Phys. Rev. B* **1988**, *37*, 9703.
(42) Fletcher, J. T.; Therien, M. J. *Inorg. Chem.* **2002**, *41*, 331.
(43) Fletcher, J. T.; Therien, M. J. *J. Am. Chem. Soc.* **2002**, *124*, 4298.
(44) Weil, J. A.; Bolton, J. R.; Wertz, J. E. *Electron Paramagnetic Resonance*; J. Wiley and Sons: New York, 1994.
(45) Bencini, A.; Gatteschi, D. *EPR of Exchange Coupled Systems*; Springer-Verlag: New York, 1990.
(46) Thurnauer, M. C.; Katz, J. J.; Norris, J. R. *Proc. Natl. Acad. Sci., U.S.A.* **1975**, *72*, 3270.
(47) Swanson, L. S.; Lane, P. A.; Shinar, J.; Wudi, F. *Phys. Rev. B* **1991**, *44*, 10617.
(48) Shinar, J. *Synth. Met.* **1996**, *78*, 277.
(49) Swanson, L. S.; Shinar, J.; Yoshinao, K. *Phys. Rev. Lett.* **1990**, *65*, 1140.
(50) Gouterman, M. *J. Mol. Spectrosc.* **1961**, *6*, 138.
(51) Karki, L.; Vance, F. W.; Hupp, J. T.; LeCours, S. M.; Therien, M. J. *J. Am. Chem. Soc.* **1998**, *120*, 2606.
(52) LeCours, S. M.; DiMagno, S. G.; Therien, M. J. *J. Am. Chem. Soc.* **1996**, *118*, 11854.
(53) Susumu, K.; Angiolillo, P. J.; Therien, M. J. Manuscript in preparation, 2003.
(54) Schmidt, J. Spin−Lattice and Spin−Spin Relaxation in Photoexcited Triplet States in Molecular Crystals. In *Relaxation Processes in Molecular Excited States*; Funfschilling, F., Ed.; Kluwer Academic Publishers: Dordrecht, The Netherlands, 1989; p 3.
(55) Gradl, G.; Friedrich, J. *Phys. Rev. B* **1987**, *35*, 4915.
(56) Gradl, G.; Friedrich, J.; Kohler, B. E. *J. Chem. Phys.* **1986**, *84*, 2079.
(57) Gradl, G.; Friedrich, J. *Chem. Phys. Lett.* **1985**, *114*, 543.
(58) Bennati, M.; Grupp, A.; Mehring, M.; Bauerle, P. *J. Phys. Chem.* **1996**, *100*, 2849.
(59) Bennati, M.; Nemeth, K.; Surjan, P. R.; Mehring, M. *J. Chem. Phys.* **1996**, *105*, 4441.
(60) Bennati, M.; Grupp, A.; Mehring, M.; Nemeth, K.; Surjan, P. R.; Bauerle, P. *Synth. Met.* **1997**, *84*, 607.
(61) Beljonne, D.; Cornil, J.; Friend, R. H.; Janssen, R. A. J.; Brédas, J. L. *J. Am. Chem. Soc.* **1996**, *118*, 6453.
(62) Warman, J. M.; Gelinck, G. H.; Piet, J. J.; Suykerbuyk, J. W.; De Haas, M. P.; Langeveld-Voss, B. M.; Janssen, R. A.; Hwang, D.-H.; Holmes, A. B.; Remmers, M.; Neher, D.; Müllen, K.; Bauerle, P. *Proc. SPIE* **1997**, *3145*, 142.
(63) Angiolillo, P. J.; Uyeda, H. T.; Therien, M. J. Unpublished results.